数理解析研究所講究録
第 739 巻 1991 年 148-164


# Dynamics of Convection in Binary Fluid Mixtures

Hideo YAHATA

Department of Materials Science, Faculty of Science
Hiroshima University, Hiroshima 730

The Rayleigh-Bénard convection in a binary fluid mixture is studied using a model system of coupled-mode equations for several chosen sets of the external parameters. The field variables are assumed to be two-dimensional and periodic in the horizontal direction. The velocity, the temperaure and the concentration variables obey the rigid, isothermal and impermeable boundary conditions on the horizontal surfaces respectively. The system with increase of the Rayleigh number develops periodic, quasi-periodic and non-periodic travelling waves of the convection rolls one after another. In particular, the non-periodic waves change the direction of propagation with irregular time intervals.

## §1. Introduction

The Rayleigh-Bénard convection occurring in a binary fluid mixture confined between two horizontal parallel plates heated from below has recently attracted considerable interest both experimentally and theoretically. Depending on the chosen set of the values of control parameters, there are cases where the system exhibits behavior of convection in several respects quite different from that usually observed in ordinary one-component fluids.[1)~7)] First, with increase of the Rayleigh number or the vertical thermal gradient across the fluid, the heat conduction state loses its stability by the subcritical Hopf bifurcation. Second, the convection rolls arising as a result of this bifurcation for some cases take the form of a spatially localized state, which thereby gives rise to coexistence of the convection and conduction states in the same vessel. Third, the convection rolls quite often move in one direction or the other in the form of travelling waves. It is further to be noted that the results given above are all observed for a range of the Rayleigh numbers near the onset of convection.

In order to clarify these conspicuous properties of the system, a variety of theoretical attempts have been made.[8)~15)] In particular, time evolution of the convection rolls were studied with the aid of the Galërkin mode truncation or the finite difference scheme applied to the basic equations of motion. The results of these computations show that the system exhibits various types of oscillatory motion in the form of standing, travelling, modulated travelling and chaotic waves of the convection rolls. These are considered to illustrate some facets of rich dynamical properties inherent in the original fluid system. Incidentally, most experiments were performed using an ethanol-water mixture confined in a rectangular cell. By contrast, in order to remove the side-wall effect on formation of the convection rolls, experiments using an annular cell have been carried out by at least two research groups.[6),7)] For this case, the convection is considered to obey the periodic boundary condition in the azimuthal direction.

Furthermore, the ratio of the cell width to the annular radius is set to be sufficiently small to such a degree that the effect of the cell curvature on the wave motion can be neglected.

The purpose of the present paper is to study time behavior of the periodic rolls using a Galërkin system of equations under the external conditions similar to those imposed on the annular-cell experiments given above. Hence, the field variables are assumed to be periodic in the azimuthal direction. We further assume that the field variables are uniform in the radial direction so that their dependece on the radial coordinate is discarded. Since the system is mainly dealt with near the onset of convection, it does not appear that complicated nodal structure in the radial direction needs to be taken into account in our computation. The system is thus assumed to be two dimensional. Similar types of the Galërkin equations were used by several authors to study evolution of the convection rolls under different external conditions.[10),12)]

In §2 formulation of the problem is given to present the model equations of motion. In §3 computational results are given for several chosen values of the external parameters suitable for comparison with those of the experiments. Finally, §4 is devoted to a short summary.

## §2. Basic equations of motion

We consider a binary fluid confined between two horizontal parallel plates heated from below. Let $x$, $y$ and $z$ denote the rectangular Cartesian coordinates with the $z$ axis directed upward. The physical quatities used in this paper are defined as follows: $\rho$ is the density of fluid, $C_p$ is the specific heat per unit mass at constant pressure, $\nu$ is the kinematic viscosity, $\kappa$ is the thermal diffusivity, $\alpha$ is the thermal expansion coefficient, $\beta$ is the solutal expansion coefficient, $D$ is the diffusion coefficient of the

component 1, $g$ is the gravitational constant, $d$ is the depth of the fluid layer and $T_d$ is the temperature difference between the two horizontal boundaries. In addition to the velocity, the pressure and the temperature, another field variable, i.e., the mass fraction of the fluid component $x_1$ is needed to specify the dynamical states of binary fluids. The heat and mass flux are $\mathbf{q} = -C_p\rho\kappa\nabla T - C_p\rho\gamma_1\nabla x_1, \mathbf{j}_1 = -\rho\gamma_2\nabla T - \rho D\nabla x_1$ where the terms containing $\gamma_1$ and $\gamma_2$ represent the Dufour and the Soret effect respectively. The term due to the Dufour effect is henceforth neglected since $\mathbf{q}$ is for cases of liquids dominated by the thermal conduction term. For the non-dimensional description of the equations of motion, the length scale $d$, the time scale $d^2/\kappa$, the temperature scale $\kappa\nu/g\alpha d^3$ and the concentration scale $\kappa\nu\gamma_2/g\alpha d^3 D$ are used. Within the framework of the Boussinesq approximations, binary fluid convection is governed by the disturbance equations for the velocity $\mathbf{u}=(u_x, u_y, u_z)$, the temperature $\theta$, the mass concentration $\xi_1$ and the pressure $\delta p$. Using the variable $\eta = \xi_1 + \theta$ instead of $\xi_1$, these are expressed in the form

$$\partial_t u_i - \sigma \triangle u_i - \sigma\{(1+S)\theta - S\eta_1\}\delta_{i,z} + \partial_i(\delta p/\rho) = -u_j\partial_j u_i, \quad (i = x, y, z) \tag{1}$$

$$\partial_t\theta - \triangle\theta - Ra\, u_z = -u_j\partial_j\theta \tag{2}$$

$$\partial_t\eta - \triangle\theta - L\triangle\eta = -u_j\partial_j\eta \tag{3}$$

$$\partial_j u_j = 0 \tag{4}$$

where $Ra = g\alpha d^3 T_d/\kappa\nu$ is the Rayleigh number, $\sigma = \nu/\kappa$ is the Prandtl number, $L = D/\kappa$ is the Lewis number and $S = \beta\gamma_2/\alpha D$ is the separation ratio while $\delta_{i,j}$ is Kronecker's delta. We solve the problem under the following conditions. On the horizontal surfaces the field variables $\mathbf{u}$, $\theta$ and $\eta$ obey the rigid(non-slip), isothermal and impermeable boundary conditions respectively:

$$\mathbf{u} = \partial_z u_z = \theta = \partial_z\eta = 0 \quad \text{on} \quad z = \pm 1/2 \tag{5}$$

Convection is now assumed to appear in the form of parallel rolls and to be spatially periodic in the $x$-axis direction perpendicular to the roll axis (parallel to the $y$ axis). Furthermore, the convection rolls are assumed to be two-dimensional. Hence, the field variables depend only on the variables $x$, $z$ and $t$. The two dimensional flow $\mathbf{u}$ is expressed in terms of the stream function $\Phi(x,z,t)$:

$$u_x = -\partial_z \Phi, \quad u_y = 0, \quad u_z = \partial_x \Phi \tag{6}$$

Substitution of Eq. (6) in Eqs. (1)$\sim$(4) gives rise to the equations of motion for $\Phi$, $\theta$ and $\eta$:

$$\partial_t \triangle_2 \Phi + \sigma \triangle_2^2 \Phi - \sigma\{(1+S)\partial_x \theta - S\partial_x \eta\} = -(\partial_x \Phi)(\partial_z \triangle_2 \Phi) + (\partial_z \Phi)(\partial_x \triangle_2 \Phi) \tag{7}$$

$$\partial_t \theta - \triangle_2 \theta - Ra\ (\partial_x \Phi) = (\partial_z \Phi)(\partial_x \theta) - (\partial_x \Phi)(\partial_z \theta) \tag{8}$$

$$\partial_t \eta - \triangle_2 \theta - L\ \triangle_2\ \eta = (\partial_z \Phi)(\partial_x \eta) - (\partial_x \Phi)(\partial_z \eta) \tag{9}$$

with $\triangle_2 = \partial_x^2 + \partial_z^2$. Next, the two-dimensional field variables $\Phi, \theta, \eta$ are approximated by the finite sum of the orthogonal functions satisfying the associated boundary conditions

$$\Phi(x,z,t) = \sum_{\epsilon=\pm 1} \sum_{\ell=1}^{L} \sum_{n=1}^{N} P_{\epsilon,\ell,n}(t) f_\epsilon(\ell a x) \varphi_n(z) \tag{10}$$

$$\theta(x,z,t) = \sum_{\epsilon=\pm 1} \sum_{\ell=1}^{L} \sum_{n=1}^{N} T_{\epsilon,\ell,n}(t) f_\epsilon(\ell a x) \chi_n(z) \tag{11}$$

$$\eta(x,z,t) = \sum_{\epsilon=\pm 1} \sum_{\ell=1}^{L} \sum_{n=1}^{N} E_{\epsilon,\ell,n}(t) f_\epsilon(\ell a x) \psi_n(z) \tag{12}$$

where $L$ and $N$ are the number of truncation, $a$ is the wavenumber of the rolls while $f_\epsilon(x) = \cos(x)$ for $\epsilon = 1$; $= \sin(x)$ for $\epsilon = -1$. In the present work, the expansion functions $\varphi_n$, $\chi_n$, $\psi_n$ are obtained as the solutions for the eigenvalue equations on the domain $(-1/2, 1/2)$

$$(\partial_x^4 - \alpha_n^4)\varphi_n = 0, \quad \varphi_n(\pm 1/2) = \partial_x \varphi_n(\pm 1/2) = 0 \tag{13}$$

$$(\partial_x^2 + \beta_n^2)\psi_n = 0, \quad \partial_x \psi_n(\pm 1/2) = 0 \tag{14}$$

$$(\partial_x^2 + \gamma_n^2)\chi_n = 0, \quad \chi_n(\pm 1/2) = 0 \tag{15}$$

where $\alpha_n$, $\beta_n$, $\gamma_n$ denote the corresponding eigenvalues for $n = 1, 2, ..., N$. With the aid of the Galërkin procedure, we obtain a system of ordinary differential equations governing time evolution of the mode amplitudes $X = \{P_{\epsilon,\ell,n}(t), T_{\epsilon,\ell,n}(t), E_{\epsilon,\ell,n}(t)\}$

$$\partial_t X = F(X) = L(X) + N(X, X) \tag{16}$$

or, more precisely,

$$\partial_t X_p = F_p(X) = \sum_{p'} L_{p,p'} X_{p'} + \sum_{p'} \sum_{p"} N_{p;p',p"} X_{p'} X_{p"} \tag{17}$$

for $p = 1, 2, ..., N_t$ with $N_t$ denoting the total number of the retained mode variables.

## §3. Computational results

In this paper, we deal with a truncated model whose field variables are approximated by

$$\Phi(x, z, t) = \sum_{\ell=1}^{L} \sum_{n=1}^{N} \{P_{1,\ell,ne}(t) \cos[(2\ell - 1)ax]\varphi_{ne}(z) + P_{-1,\ell,ne}(t) \sin[(2\ell - 1)ax]$$

$$\times \varphi_{ne}(z) + P_{1,\ell,no}(t) \cos(2\ell ax)\varphi_{no}(z) + P_{-1,\ell,no}(t) \sin(2\ell ax)\varphi_{no}(z)\} \tag{18}$$

$$\theta(x, z, t) = \sum_{n=1}^{N} [\sum_{\ell=1}^{L} \{T_{1,\ell,ne}(t) \cos[(2\ell - 1)ax]\chi_{ne}(z)$$

$$+ T_{-1,\ell,ne}(t) \sin[(2\ell - 1)ax]\chi_{ne}(z) + T_{1,\ell,no}(t) \cos(2\ell ax)\chi_{no}(z)$$

$$+ T_{-1,\ell,no}(t) \sin(2\ell ax)\chi_{no}(z)\} + T_{1,0,no}(t)\chi_{no}(z)] \tag{19}$$

$$\eta(x, z, t) = \sum_{n=1}^{N} [\sum_{\ell=1}^{L} \{E_{1,\ell,ne}(t) \cos[(2\ell - 1)ax]\psi_{ne}(z)$$

$$+E_{-1,\ell,ne}(t)\sin[(2\ell-1)ax]\psi_{ne}(z)+E_{1,\ell,no}(t)\cos(2\ell ax)\psi_{no}(z)$$

$$+E_{-1,\ell,no}(t)\sin(2\ell ax)\psi_{no}(z)\}+E_{1,0,no}(t)\psi_{no}(z)] \qquad (20)$$

where the suffices $e$ and $o$ represent even and odd respectively. The truncation numbers are chosen to be such that $L = 2$ and $N = 2$. The system thus contains 52 mode variables in all, i.e., $N_t = 52$.

The present model system is considered to describe convection rolls extending periodically along the azimuthal direction in the entire annular cell. To our knowledge, there are two cases where experiments on binary fluid convection have been performed using annular cells. Hence, we here study the dynamical preperties of our model equations for the two cases where the values of the model parameters are specified in the same way as those used in these experiments. The first case referred to as A is associated with the experiment due to Kolodner, Bensimon and Surko(KBS) using the 8 wt-% ethanol in water at $T \simeq 27°$C where the system is specified by $\sigma = 9.7$, $L = 0.0068$, $S = -0.266$, $a = 2.86$ and $d = 0.241$ cm.[6] The second case B is the one due to Kato and Sawada(KS) using the 24 wt-% ethanol in water at $T \simeq 20°$C where the system is specified by $\sigma = 18$, $L = 0.015$, $S = -0.11$, $a = 2.89$ and $d = 0.315$ cm.[7] The vertical thermal gradient across the system is henceforth expressed in terms of $r = Ra/(Ra)_c$ with $(Ra)_c$=1708.

3.1 Case A.

First, we find the steady states of Eq.(16) $F(X) = 0$ using the Newton method for a range of the values of $Ra$ near the onset of convection. The result is shown in Fig. 1 in terms of the steady state value of the mode $P_{1,1,1e}$. The solution of the finite-amplitude convection consists of two branches constituting multiple-steady states. It is found that the lower branch is always unstable and that the upper one becomes unstable above $r = r_c = 1.17$ through the supercritical Hopf bifurcation. With increase of $r$, the convection-free state dominated by thermal conduction and

concentration diffusion loses its stability at $r = r_{os} = 1.38$ due to the subcritical Hopf bifurcation. Incidentally, KBS gives the result: $r_{os} = 1.412$. Above $r_{os}$, the mode amplitudes begin to grow indefinitely because the nonlineariy associated with the instability provides no saturation. When the amplitudes become sufficiently large, the motion tends to the stable oscillating state which winds around the unstable upper steady state arising from the supercritical Hopf bifurcation above $r = r_c = 1.17$. We next show the dynamical behavior of this oscillating state for several values of $r$. Figures 2 show time evolution of the fundamental mode amplitudes for the temperature $T_{1,1,1e}(t)$ and $T_{-1,1,1e}(t)$ at $r = 1.2, 1.3$ and $1.5$. This clearly indicates that the motion is in the state of a travelling wave in that the phase difference between the above two amplitudes is just $\pi/2$. In addition, the PSD for $T_{1,1,1e}(t)$ in Fig. 3 show that the motion is periodic at $r = 1.2$, quasi-periodic at $r = 1.3$, and non-periodic at $r = 1.5$. In the KBS experiment, the period of the extended travelling wave gradually increases from 5 to 250 $d^2/\kappa$ over a range of $r$ from 1.250 to 1.412.[6] By contrast, in our model the wave propagates with almost the same period $\sim 4\ d^2/\kappa$ over a range of $r$ around $r_{os}$. In order to show the travelling-wave state in more detail, the periodic pattern of the roll state is depicted in Fig. 4 for successive values of time. The wave patterns are found to move with lapse of time. In particular, it is found that at $r = 1.5$ the abrupt alternation of the direction of the wave propagation occurs quite irregularly.

3.2 Case B.

For the case where the external parameters are the same as those in KS experiment, the steady states are determined in such a way as shown in Fig. 5. First it is to be noted that the system is unstable on the lower branch of its steady convection state. When $r$ is increased, the thermal conduction state becomes unstable at $r = r_{os} = 1.17$ through the subcritical Hopf bifurcation. In contrast to Case A, however, the upper branch of the steady state solution remains stable over a wide range of the values of

$r$ around $r_{os}$, and loses its stability at the Rayleigh number as high as $r = r_c = 2.10$. Hence, the system point which above $r_{os}$ departs from the unstable convection-free state tends to the stable steady state represented by the upper-branch of the steady solutions. In this sense, the extended oscillating state does not expected to occur. If we refer to the experimental results due to KS, it appears that the oscillating convection occurs only in the form of a spatially localized state.[7] In order to give further evidence, we compute the steady state of the starting original equations (1)~(4) directly using finite-difference MAC method without relying on the Galërkin truncation procedure.[16] The results show that the solution tends to the steady state for several moderate values of $r$ above $r_{os}$. For comparison, Figs. 6 and 7 show the isopleths of the field variables $u_x, u_z, \theta$ and $x_1$ obtained by these two different procedures. Although these two give the results quite similar to each other for $u_x, u_z$ and $\theta$, marked difference in the result for $x_1$ is quite noticeable. This occurs as a result of the smallness of the coefficient $L$. It seems that the Galërkin procedure is quite ineffective in describing steep variation of the field variable near the boundary plates.

## §4. Summary and discussions

As mentioned earlier, quite a few attempts were so far made to elucidate dynamical properties of the convection rolls appearing in binary fluid mixtures. Among others, the Lorentz model was extended to describe binary fluid systems. The model needs to contain at least eight mode variables. As for the boundary conditions obeyed by the field variables, in the 8-mode model due to Cross, the velocity and the concentration variables are assumed to be free-slip and permeable on the horizontal surfaces.[10] By contast, in the 8-mode model by Linz and Lücke(LL), the horizontal boundary condition for the concentration flux is modified in such a way to satisfy the impermiability.[12]

If the expansion functions in Eqs. (10)$\sim$(12) are suitably chosen to satisfy the boundary conditions given above, the eight mode variables included in the model are given by $P_{1,1,1e}, P_{-1,1,1e}, T_{1,1,1e}, T_{-1,1,1e}, T_{1,0,1o}, E_{1,1,1e}, E_{-1,1,1e}, E_{1,0,1o}$. It seems that the LL model gives the results in several respects quite similar to that of ours presented as Case A of §3. If the values of the model parameters assumed in both computations are taken into account, the results of LL should be compared rather with those of ours for Case B. This is, however, impossible because the critical Rayleigh number $r_c$ for Case B is quite high due to the rigid boundary condition imposed on the velocity and the value of the wavenumber determined by the circumference of the annulus. With this reservation, it is concluded that both systems with increase of $r$ exhibit similar behaviors summarized as follows: (i) the convection-free state undergoes the subcritical Hopf bifurcation at $r = r_{os}$; (ii) the convection state represented by the upper branch of the steady state solution becomes unstable above $r = r_c$ through the supercritical Hopf bifurcation; (iii) with further increase of $r$ above $r_c$, the system falls in the modulated travelling-wave state. In our 52-mode model, the variables not included in the eight fundamental variables given above are found to take relatively small values during the system evolution. If this is taken into account, the main difference between the LL and our models lies in the boundary condition imposed on the velocity. As far as the above results show, it seems that this has no crucial influence on global dynamical behavior of convection.

On the other hand, evolution of the two-dimensional thermosolutal convection in a box was studied using a finite difference method.[13),14)] The boundary conditions were chosen in such a way that the velocities are free-slip; that the temperture as well as the concentration is fixed and insulating (or impermeable) on the horizontal and the side walls respectively. The computational results show that convection exhibits a variety of spatio-temporal behavior in the form of travelling, standing, modulated

travelling and chaotic waves. Furthermore, the travelling waves were found to reverse their direction of propagation with irregular time intervals.[14] This result has a marked resemblance to that occurring in propagation of the travelling waves of our model, although the relevant travelling waves in our models are basically sustained in the modulated (or quasi-periodic) state. However, we have thus far not clarified in our model the mechanism underlying this reversal phenomenon. Incidentally, Funakoshi and Inoue carried out a series of experiments on surface waves in a cylindrical container subject to horizontal periodic forced oscillations.[17] They discovered that chaotic waves under certain conditions reverse their direction of propagation along the circumference. It is not clear if this has any relevance with the above-mentioned similar results for binary mixtures.

The model used in this paper applies to the convection rolls extending in the entire annulus because of their assumed periodicity in the $x$ direction. In actual experiments, however, the rolls extending only over a limited region of the container are more prevalently observed in both rectangular and annular cells. It appears at present that no remarkable progress has been made in theoretically understanding emergence and evolution of the spatially localized convection state.

## Acknowledgements

The author wishes to express his gratitude to Professor Y. Sawada and Mr. T. Kato for helpful discussions and showing him their experimental data prior to publication.

## References

1) D.T.J. Hurle and E. Jakeman, J. Fluid Mech. **47**(1971), 667.

2) D. Gutkowicz-Krusin, M.A. Collins and J. Ross, Phys. Fluids **22**(1979), 1443,1451.

3) R.W. Walden, P. Kolodner, A. Passner and C.M. Surko, Phys. Rev. Lett. **55**(1985), 496.

4) E. Moses, J. Fineberg and V. Steinberg, Phys. Rev. **35A**(1987), 2757.

5) R. Heinrichs, G. Ahlers and D.S. Cannell, Phys. Rev. **35A**(1987), 2761.

6) P. Kolodner, D. Bensimon and C.M. Surko, Phys. Rev. Lett. **60**(1988), 1723.

7) T. Kato and Y. Sawada, private communications.

8) E. Knobloch, Phys. Rev. **34A**(1986), 1538.

9) M.C. Cross, Phys. Rev. Lett. **57**(1986), 2935.

10) M.C. Cross, Phys. Lett. **A119**(1986), 21.

11) E. Knobloch, A.E. Deane, J. Toomre and D.R. Moore, Contemporary Mathematics **56**(1986), 203.

12) S.J. Linz and M. Lücke, Phys. Rev. **35A**(1987), 3997.

13) A.E. Deane, E. Knobloch and J. Toomre, Phys. Rev. **36A** (1987), 2862.

14) A.E. Deane, E. Knobloch and J. Toomre, Phys. Rev. **37A** (1988), 1817.

15) W. Barton, M. Lücke, W. Hort and M. Kamps, preprint.

16) R. Peyret and T.D. Taylor, *ComputationalMethodsforFluidFlow*, (Springer, 1983).

17) M. Funakoshi and S. Inoue, J. Fluid Mech. **192**(1988), 219.

## Figure Captions

Fig. 1. The solution $X = P_{1,1,1e}$ representing steady convection states for Case A as a function of $r$ where $r_{os} = 1.38$ and $r_c = 1.17$.

Fig. 2. Time evolution of the mode amplitudes $T_{1,1,1e}(t)$ (full line) and $T_{-1,1,1e}(t)$ (dashed line) for Case A with (a) $r = 1.2$, (b) $r = 1.3$, (c) $r = 1.5$.

Fig. 3. The PSD for $T_{1,1,1e}(t)$ for Case A where the abscissa measures the frequency in unit of $10\kappa/d^2$; (a) $r = 1.2$, (b) $r = 1.3$, (c) $r = 1.5$.

Fig. 4. Spatial patterns of the temperture field for Case A at $r = 1.5$ and $z = 0.2$ as a function of position along the $x$ direction at time intervals $0.032d^2/\kappa$. Time increases in the upward direction: (a) the rolls drift in the same direction, (b) the wave reverses the direction of propagation.

Fig. 5. The solution $X = P_{1,1,1e}$ representing steady convection states for Case B as a function of $r$ where $r_{os} = 1.17$.

Fig. 6. The isopleths for (a) $u_x$, (b) $u_z$, (c) $\Theta$, and (d) $\xi_1$ drawn in the $(x, z)$-planes at $r = 1.4$, where $\Theta$ represents the sum of the disturbance field $\theta$ and the steady temperature field with a linear profile in the vertical direction. The results are obtained using the 52-mode model given in the present paper.

Fig. 7. The same as in Fig. 6 except that the results are obtained by the finite-difference MAC method.

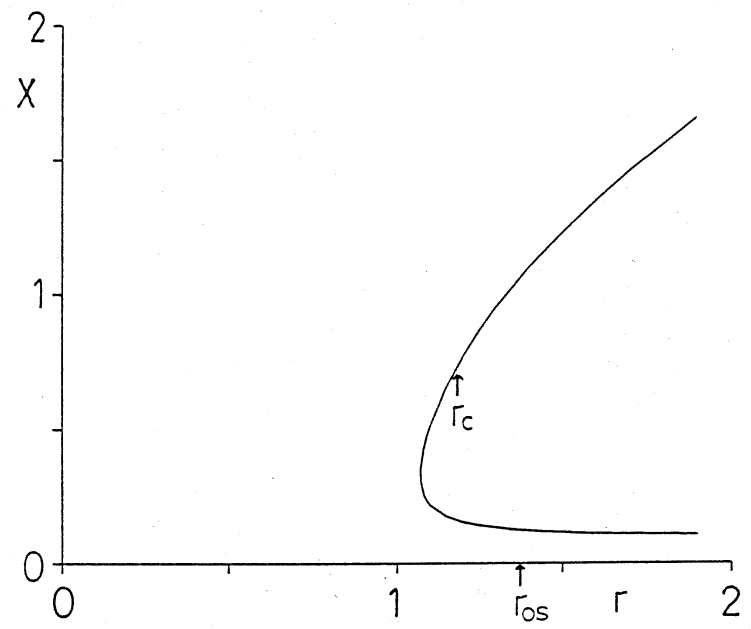


Fig. 1

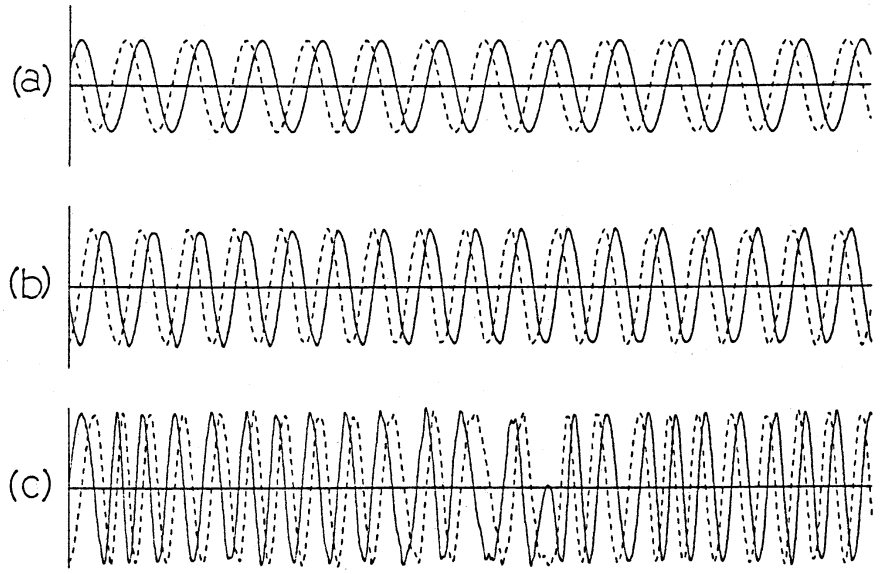


Fig. 2

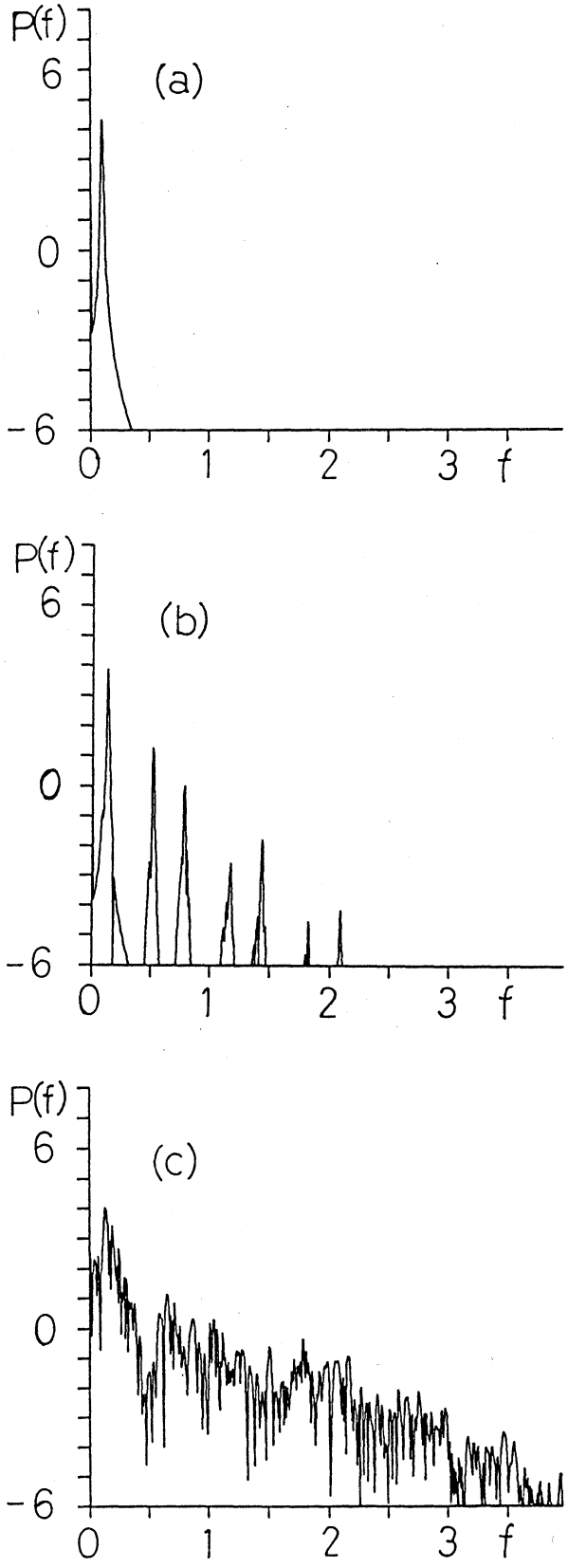


Fig. 3

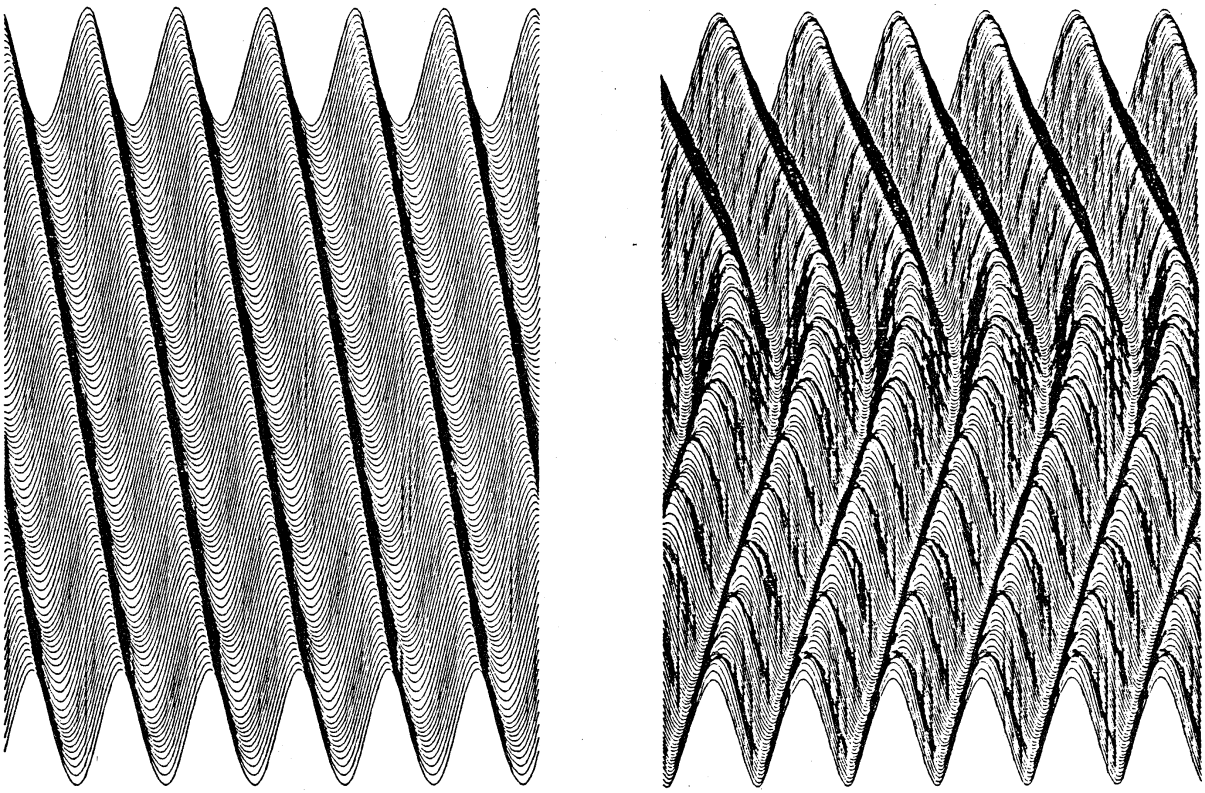

Fig. 4 (a) (b)

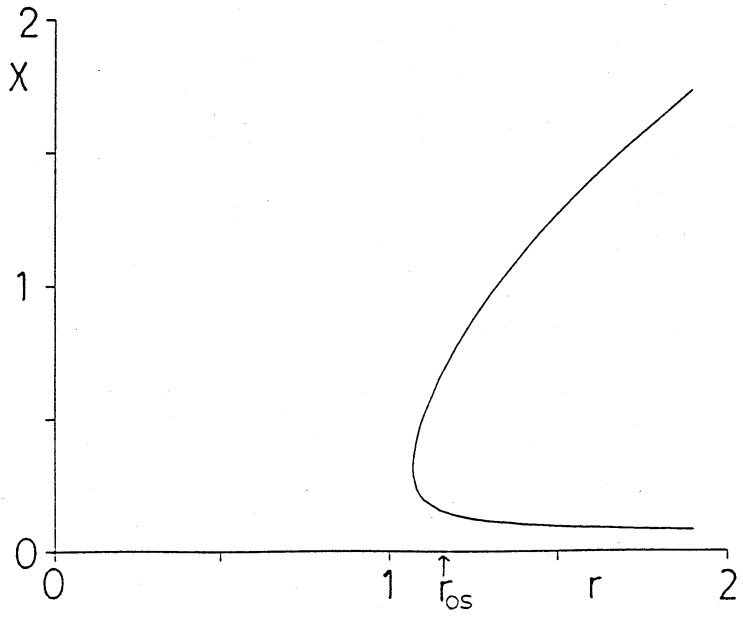


Fig. 5

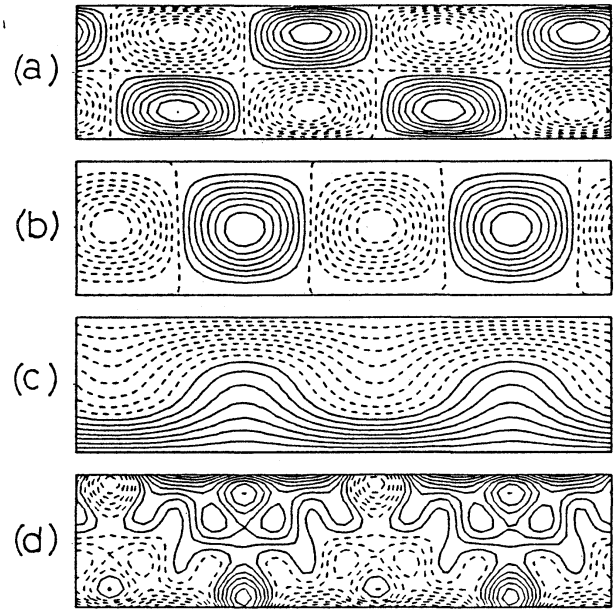


Fig. 6

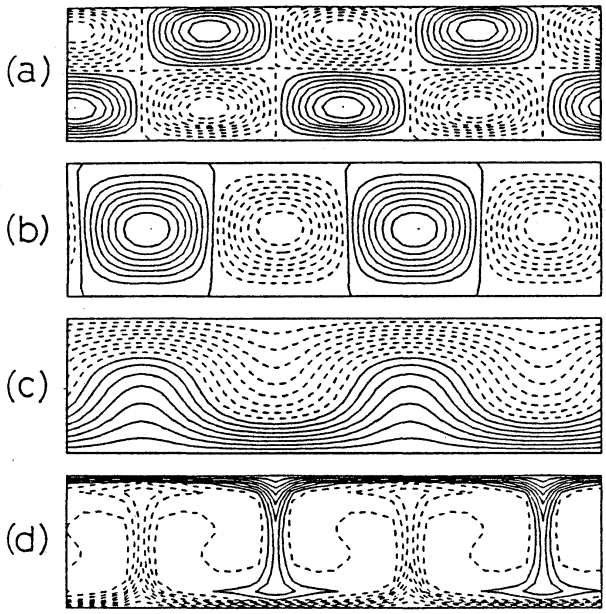


Fig. 7